Cell Reports, Volume *24*

Supplemental Information

Joint Representation of Spatial and Phonetic Features in the Human Core Auditory Cortex

Prachi Patel, Laura K. Long, Jose L. Herrero, Ashesh D. Mehta, and Nima Mesgarani

Supplemental Materials

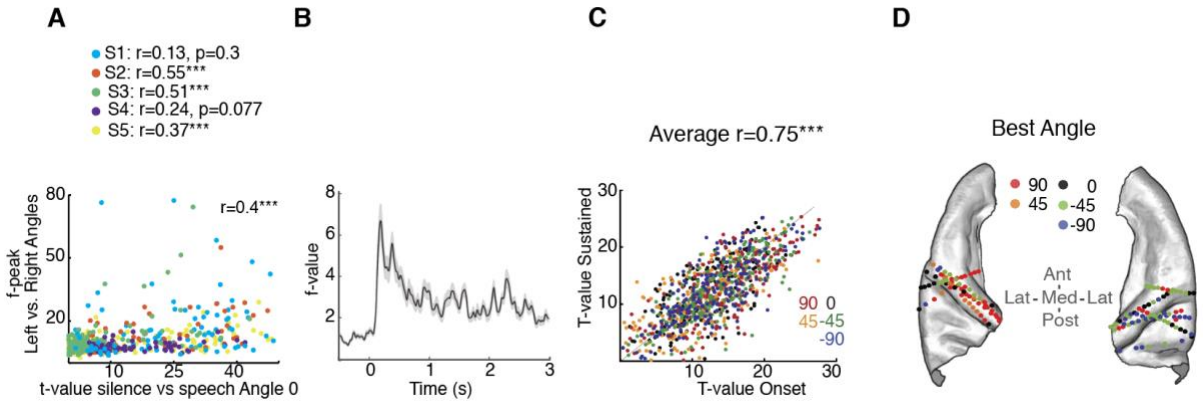

Figure S1. Related to main Figure 1. (A) Scatter of maximum f-statistic between left- versus right-sided angles (measuring amount of spatial information) versus t-value between silence and speech (measuring speech responsiveness) colored by subject number. The correlation between the two measures indicate that speech responsive electrodes were spatially selective (r=0.4, p<0.001). (B) F-statistic of neural response between left- versus right-sided angles over time. (C) T-values from onset (0-0.5s, from Figure S1A) and sustained parts (1-1.5s, from Figure S1A) of the response are highly correlated. (D) Best Angle (BA) on ICBM152 average brain.

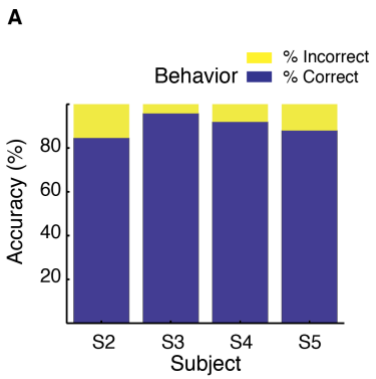

Figure S2. Subject behavior related to Method details section. (A) Accuracy in reported behavior for four subjects.

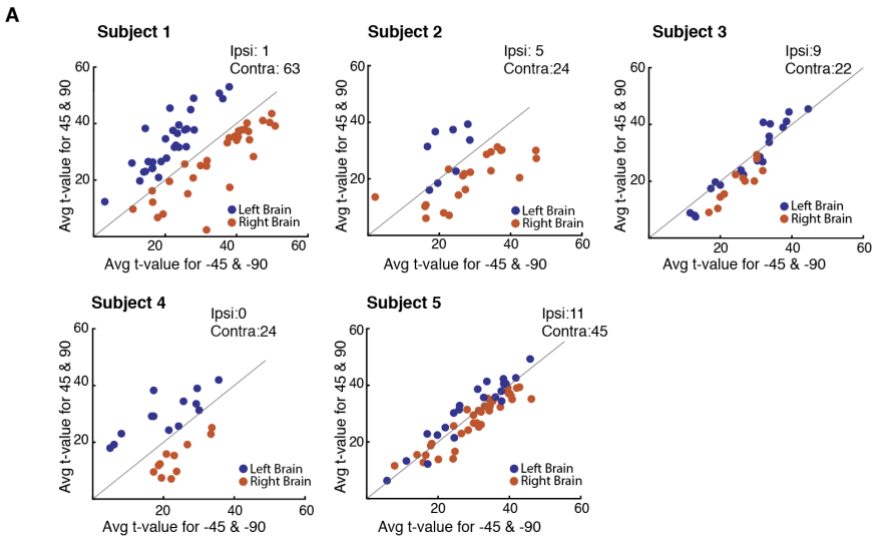

Figure S3. Related to main Figure 2. (A) Analysis from Figure 2A for each subject.

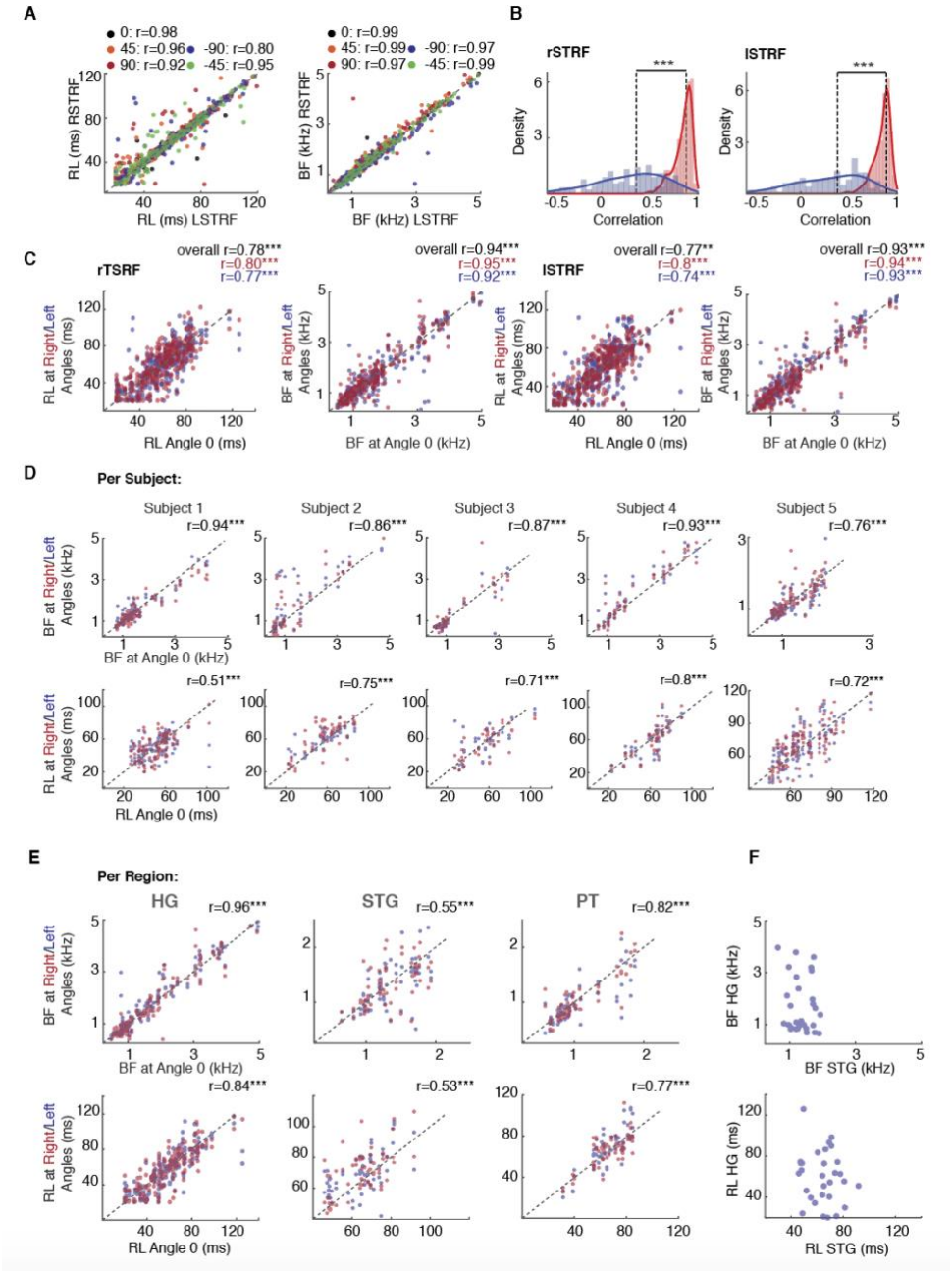

Figure S4. Related to main Figure 3. (A) BF and RL from *l*STRF and *r*STRF are highly correlated. The x-axis shows BF/RL from *l*STRF and the y-axis shows BF/RL from *r*STRF, colored by angle. Correlation values are as noted, P<0.001. (B) Analysis from Figure 3C using *l*STRF and *r*STRF, replicating the result that correlation between STRFs from same electrode and different angle is significantly higher than correlation between STRFs from different electrode and same angle (P<0.001, Wilcoxon ranksum test). (C) Analysis from Figure 3D using *l*STRF and *r*STRF replicating the result that tuning properties and angles are independently encoded. (D) Analysis from Figure 3D divided per subject. (E) Analysis from Figure 3D divided per brain region. (F) Relationship between BF and RL in the areas of HG and STG.

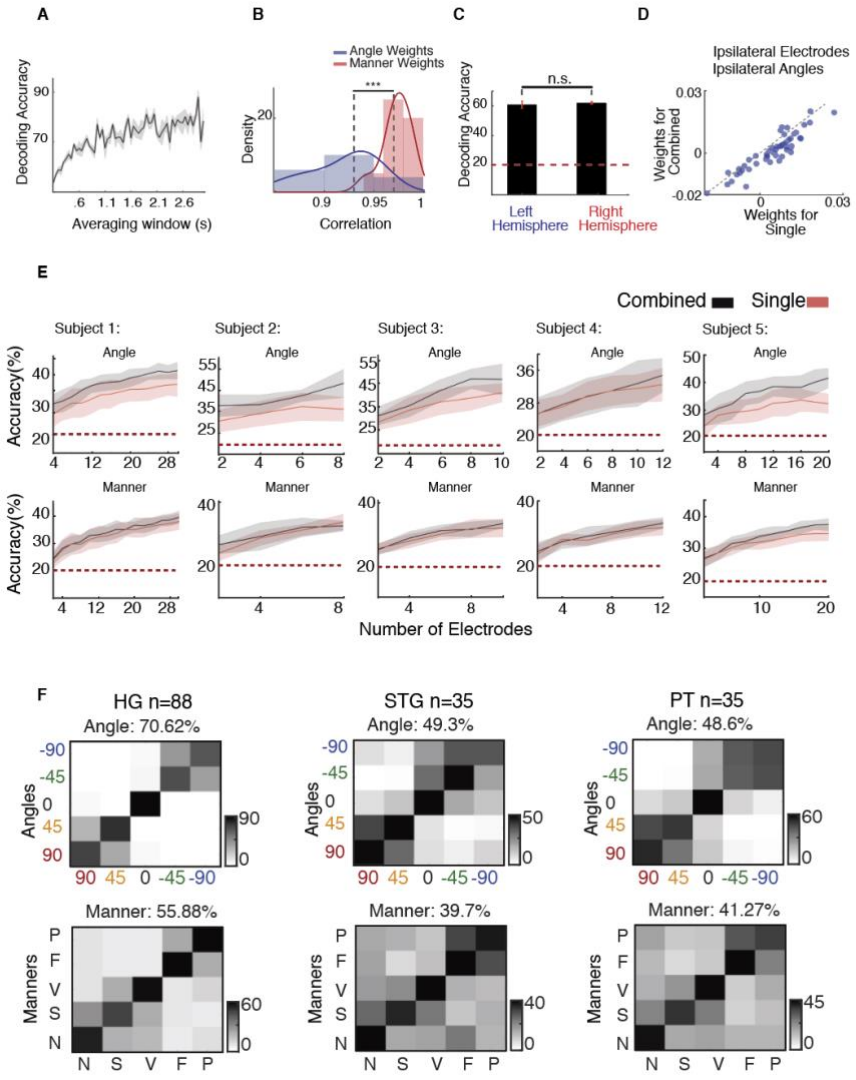

Figure S5. Related to main Figure 4. (A) Decoding accuracy (y-axis) from 10 cross-validations for different time windows (x-axis); there is a gradual rise in accuracy as window size increases up to 1.5s. (B) Histograms of correlation values of weights obtained from single hemispheres with those from both brain hemispheres. Correlation between weights of single and both hemispheres was found to be significantly higher for manner decoding than for angle decoding ($P<0.001$, Wilcoxon ranksum test). (C) Angle decoding accuracy using only left and only right brain hemisphere ($P>0.05$, unpaired t-test). (D) For decoding of the ipsilateral angles, the ipsilateral electrodes have higher normalized weights for single hemispheric decoding as compared to combined hemispheric decoding. (E) Analysis from Figure 4B broken down per subject. (F) Analysis from Figure 4A broken down per brain region.

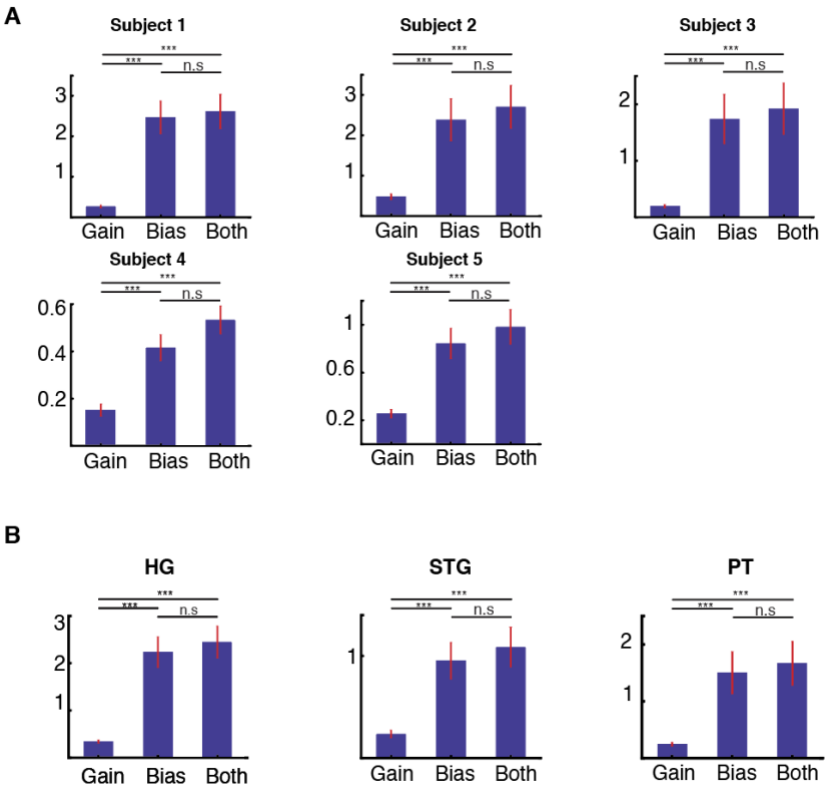

Figure S6. Related to main Figure 5. (A) Analysis from Figure 5C broken down per subject. (B) Analysis from Figure 5C broken down per brain area (HG, STG, PT).

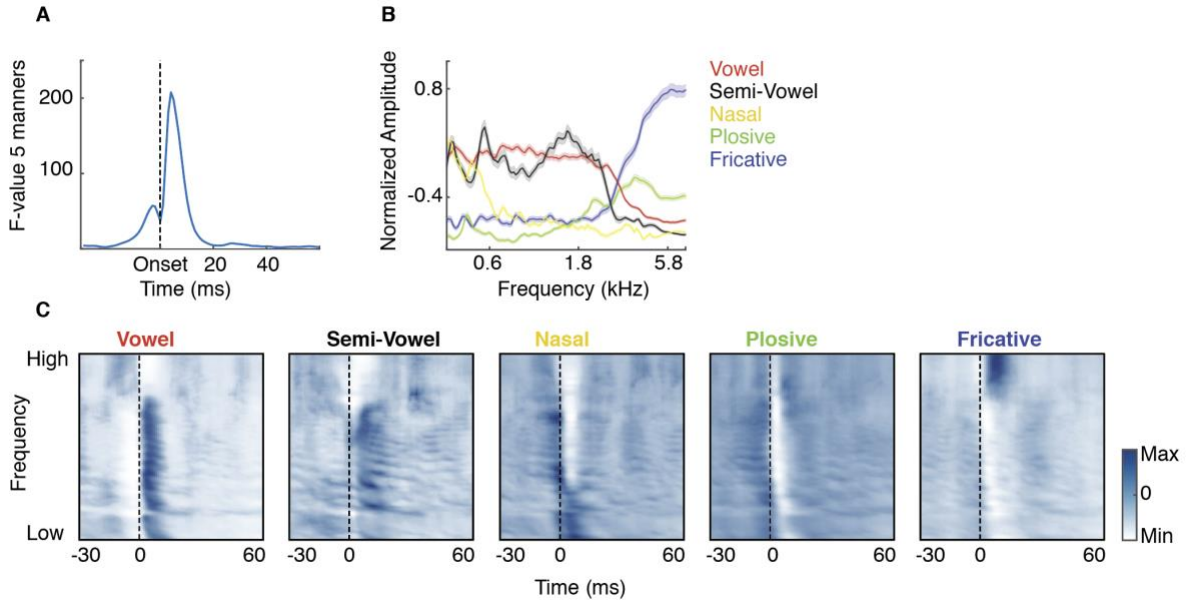

Figure S7. Acoustic properties related to main Figure 4. (A) Average F-ratio for the separation of 5 manners of articulation (plosive, fricative, vowel, nasal and semi-vowel) over time. (B) Average amplitude and standard error across phonetic utterances for the frequencies in acoustic spectrograms of five manners of articulation. (C) Average spectrograms of phonemes for each manner of articulation.

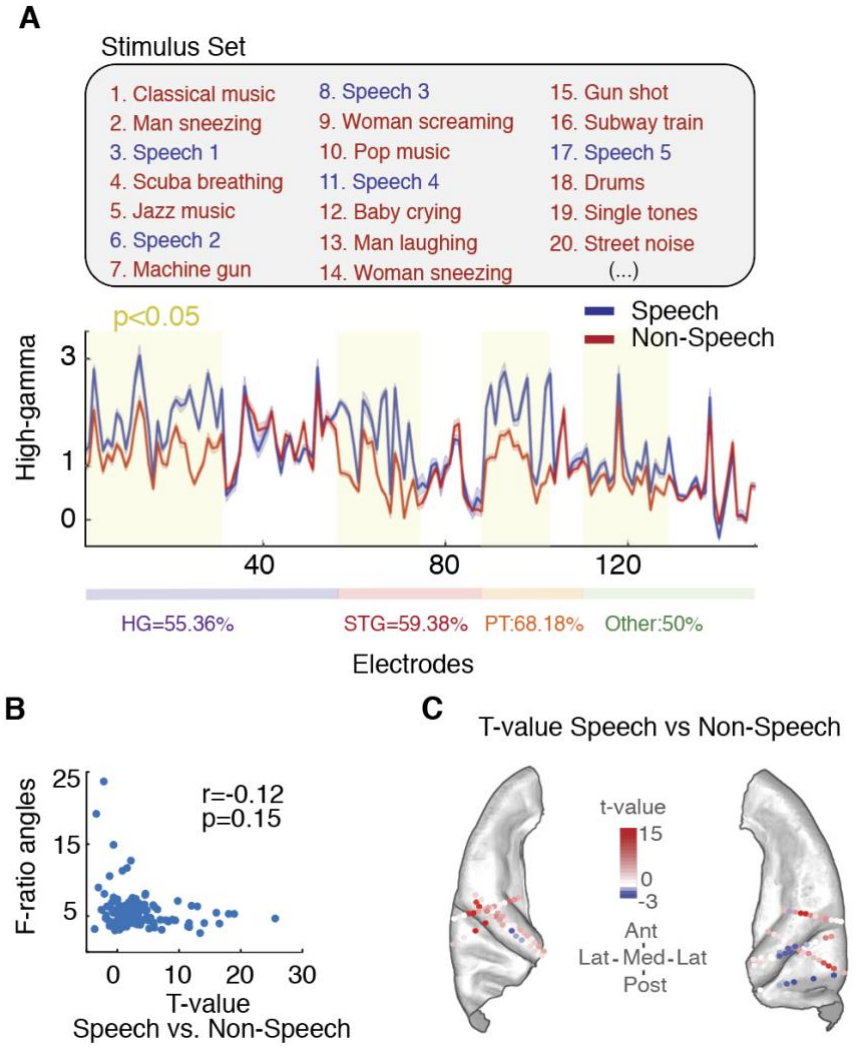

Figure S8. Speech Specificity related to main Figure 4. (A) Stimulus set with examples of various speech and non-speech sounds. Average high-gamma response (y-axis) for electrodes from 3 subjects (x-axis) show that we have coverage in areas that are selective to speech over other non-speech sounds. (B) Absence of relationship between amount of direction encoding and the amount of speech specificity. (C) Electrodes in core auditory areas colored by speech specificity.